



Computational investigation of *Pluchea indica* mechanism targeting peroxisome proliferator-activated receptor gamma



Purnawan Pontana Putra^{1*}, Raden Bayu Indradi², Tegar Achsendo Yuniarta³, Dini Hanifa¹, Mokhamad Fahmi Rizki Syaban⁴, Netty Suharti⁵

¹Departement of Pharmaceutical Chemistry, Faculty of Pharmacy, Universitas Andalas, Padang, 25163, Indonesia

²Department of Biological Pharmacy, Faculty of Pharmacy, Universitas Padjadjaran, Sumedang 45363, Indonesia

³Departement of Pharmaceutical Chemistry, Faculty of Pharmacy, University of Surabaya, Surabaya, 60293, Indonesia

⁴Faculty of Medicine, Universitas Brawijaya, Malang, 65145, Indonesia

⁵Departement of Biology Pharmacy, Faculty of Pharmacy, Universitas Andalas, Padang, 25163, Indonesia

ARTICLE INFO

Article Type:

Original Article

Article History:

Received: 16 March 2024

Accepted: 29 May 2024

published: 1 October 2024

Keywords:

Pluchea indica

Antidiabetic activity

Network pharmacology

Molecular docking

Molecular dynamics

ABSTRACT

Introduction: *Pluchea indica* is known to have diverse pharmacological properties, including anti-inflammatory, antioxidant, antimicrobial, and anticancer activities. However, there is a pressing need to thoroughly investigate the molecular interactions between *P. indica* compounds and peroxisome proliferator-activated receptor gamma (PPARG). This study aimed to elucidate the molecular mechanisms behind *P. indica* and PPARG, and its potential implications for diabetes mellitus.

Methods: The computational investigation employed Pharmacological Network pharmacology, homology modeling, deep learning docking, and molecular dynamics to explore the active compounds and targets within *P. indica* against the PPARG.

Results: Three active compounds were identified namely pinoresinol, syringaresinol, and plucheoside A, all of which complied with the Lipinski rule of five. The deep learning-based pose scores were determined as follows: Pinoresinol 0.55, syringaresinol 0.32, and plucheoside A 0.44. Additionally, protein-protein interactions were observed with PPARG and associated with the PPAR signaling pathway. Molecular dynamics simulation analysis showed the stability of the three compounds over a 100 ns period. Free energy calculations using Molecular Mechanics-Generalized Born and Surface Area (MM-GBSA) yielded ΔG values of -44.39 kcal/mol, -51.83 kcal/mol, and -40.27 kcal/mol for pinoresinol, syringaresinol, and plucheoside A, respectively.

Conclusion: *Pluchea indica* might be developed to treat various diseases, particularly those involving the PPARG signaling pathway. It suggests the possibility of being developed as a focused medication for diabetes.

Implication for health policy/practice/research/medical education:

Three active compounds found in *Pluchea indica* that could be developed into orally absorbable drugs, showing promise in treating conditions like diabetes by targeting PPARG. The study suggests that these compounds have the potential to become targeted medications, as indicated by their favorable binding energies and stability in molecular dynamics, supported further by free energy calculations.

Please cite this paper as: Putra PP, Indradi RB, Yuniarta TA, Hanifa D, Syaban MFR, Suharti N. Computational investigation of *Pluchea indica* mechanism targeting peroxisome proliferator-activated receptor gamma. J Herbm Pharm. 2024;13(4):630-639. doi: 10.34172/jhp.2024.52544.

Introduction

Pluchea indica (L.) Less. is a plant belonging to the Asteraceae family and widely distributed in warm regions such as Southeast Asia. It has a history of traditional use and exhibits pharmacological activities encompassing

antidyslipidemic, antihyperglycemic anti-inflammatory, antioxidant, antimicrobial, and anticancer properties (1-3). Additionally, the plant can also be used for antidiabetic treatment due to its lipase inhibitor effects. When used in specific quantities as an herbal supplement, *P. indica*

*Corresponding author: Purnawan Pontana Putra,
Email: purnawanpp@phar.unand.ac.id

contributed to a reduction in obesity (4). The plant showed insecticidal and herbicidal activities and has been employed in venom treatment due to its toxin-neutralizing capability (5).

Peroxisome proliferator-activated receptor gamma (PPARG) can increase insulin sensitivity and influence the insulin formation pathway (6). It is important for the development of adipose tissue (7). Network pharmacology was employed in this present study to investigate active constituent compounds and their targets against the PPARG. According to previous studies, some constituents can even synergistically affect the different targets (8,9). The advantage of this approach lies in its ability to comprehensively view the multi-component interactions of plants and the characteristics of herbal treatments against numerous proteins (10,11). Integrating network pharmacology, absorption, distribution, metabolism, excretion (ADME) prediction, homology modeling, deep learning docking, and molecular dynamics simulation, enhances the comprehensive examination of *P. indica* potential in traditional medicine, particularly for understanding the network for PPARG. Leveraging deep learning, specifically, convolutional neural networks (CNNs), can significantly advance our understanding of the interaction between *P. indica* compounds and their protein targets, emphasizing the importance of this research (12,13).

This research aims to not only unravel the intricate relationships between *P. indica* compounds and PPARG but also to pave the way for a deeper understanding of potential drug targets and relationships for diabetes medication, thyroid hormone regulation, modulation of transmembrane receptor protein tyrosine kinase activity, cancer, and regulation of the MAPK signaling pathway.

Material and Methods

Hardware

A Computer WorkStation equipped with a Ryzen 5 3600 series processor, 16 GB of RAM, a Nvidia® GTX 1660 Super graphics processing unit (GPU), and running on the Ubuntu 20.04 LTS operating system, was utilized for conducting network pharmacology, molecular docking, and molecular dynamics simulations.

Network pharmacology analysis

Network pharmacology analysis of *P. indica* was conducted using the PhytoChemical Interactions DB (PCIDB) on the website: <https://www.genome.jp/db/pcidb/>. To identify significant disease-related target groups, protein-protein interaction (PPI) data from STRING (<https://string-db.org/>) were used (14,15). The considered organism was *Homo sapiens*, and interactions with a medium confidence score >0.400 were selected.

MetaScape was employed to analyze gene lists, pathways, and enrichment analysis (<https://metascape.org/>).

The previously obtained gene list was analyzed with the *Homo sapiens* species, and enrichment analysis with parameters Min Overlap 3, *P* value cutoff 0.01, as well as Min Enrichment 1.5 was selected. The study of the input gene list included Gene Ontology (GO) Molecular Functions pathways, such as GO Biological Processes and the Kyoto Encyclopedia of Genes and Genomes (KEGG). Structural complex analysis was conducted for cellular components, while PPI data were generated and clustered using the CytoCluster tool in Cytoscape (<https://cytoscape.org/>).

Absorption, distribution, metabolism, excretion analysis

The active compound was analyzed for physicochemical descriptors and to predict ADME, pharmacokinetic properties, and BOILED-EGG parameters using SWISS ADME (<http://www.swissadme.ch>) (17,18). Moreover, toxicity was assessed using the ADMETlab 2.0 software (19).

Homology modeling and deep learning docking

The receptor employed in this simulation was the PPARG basis of heterodimerization among nuclear receptors with PDB ID: 1FM9 (20). Homology modeling was performed using SWISS-MODEL (21). Protein, native ligand separation and analysis of their interactions were achieved using the Discovery Studio 2020 software (<https://discover.3ds.com/>). Furthermore, geometry optimization was performed through the Avogadro software (22) with the Merck Molecular Force Field (MMFF94), while the Python-based cloud platform Google Colab was used for molecular docking simulations (23). Redocking was conducted to verify the docking protocol, utilizing an RMSD value of <2 for validation purposes (24). The software employed a Deep Learning algorithm (CNN) with Gnina version 1.0.3 (25). The grid box used for docking involved an autobox ligand, where the ligand file determined the binding site. This was achieved by creating a prism around the ligand with additional space added in each dimension, and the GPU used in this simulation was the Tesla T4 with CUDA version 12.0.

Molecular dynamics simulation

CHARMM-GUI was used for input file preparation for protein, native ligand, and active compound (26). Ionization was carried out with KCl at a concentration of 0.15 and the system size used was the rectangle model. Periodic boundary conditions were used with particle-mesh Ewald (PME) and fast Fourier transform (FFT). Moreover, the Amber FF19SB force field and the OPC water model were applied to protein and ligand (27). Ligand parameterization was performed using GAFF2 and hydrogen mass repartitioning was used to accelerate the simulation to 4 fs (28). Equilibration was conducted with constant number of particles, volume, and

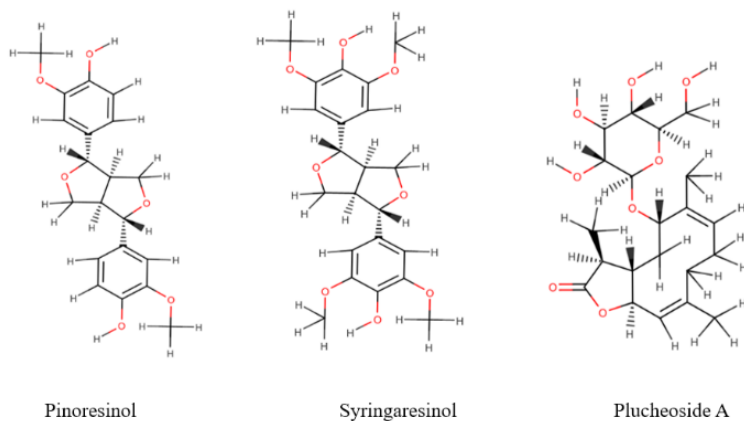


Figure 1. Active compounds of *Pluchea indica* from database PCIDB.

temperature (NVT) ensemble, followed by production simulation with constant number of particles, pressure, and temperature (NPT) ensemble at 310 K. The simulations were run using Gromacs 2022.2 software with a total time of 100 ns (29,30). Free energy calculation was carried out through MM-GBSA with gmx_MMPBSA (31,32).

Results

Three active compounds were obtained from *P. indica*, namely pinoresinol, syringaresinol, and plucheoside, as shown in Figure 1 obtained from <https://www.genome.jp/db/pcidb/>.

To comprehend the protein-protein interactions targeted by the active compounds from *P. indica*, PPI analysis was performed using string-db for the eight specific proteins. A total of 10 edges (associations) were generated from the analysis of 8 nodes (target proteins), as shown in Figure 2, with a PPI enrichment *P* value of 0.000159. This value indicated that the resulting network interacted more than a random set of proteins, suggesting these proteins were interconnected or partially connected as a group.

To find out the proteins that had interactions with PPAR γ , we performed a protein-protein interaction study by entering a web server string, which was then visualized using Cytoscape, as shown in Figure 3. Then, the proteins

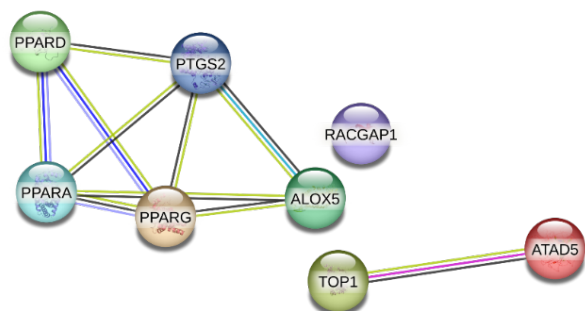


Figure 2. Protein-protein interaction network of *Pluchea indica* in which PPAR γ is connected to other proteins.

were chosen based on the density between centers, as shown in Figure 3.

The heatmap of selected GO Parents was used for the visualization and analysis of the data related to hierarchical information about gene functions and GO. GO is capable of depicting the hierarchical functions of genes and proteins in three aspects namely Biological Process, Molecular Function, and Cellular Component. Figure 4, presenting the values of $-\log_{10}(P)$, shows that the larger the value, the more significant the results.

Enrichment GO was used to identify biological pathways associated with genes. This analysis can be applied to data from various sources, including RNAi experiments, mutations, and genomic data. Figure 5 shows the interconnectedness between Transmembrane receptor protein tyrosine kinase activity, Central carbon metabolism in cancer, and the MAPK signaling pathway.

Pinoresinol, syringaresinol, and plucheoside A shared similar ADME properties as shown in Table 1. These three compounds adhered to the Lipinski rule of five for oral bioavailability, had molecular weights <500 g/mol, exhibited 5 hydrogen bond donors, 10 hydrogen bond acceptors, and a log *P* <5.

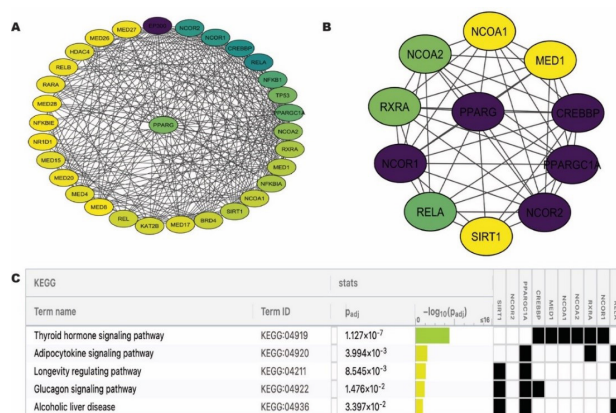


Figure 3. Protein-protein interaction network analysis. A. Network analysis from string B. Network analysis between centrality C. Signaling pathway PPAR γ relationship with thyroid hormone.

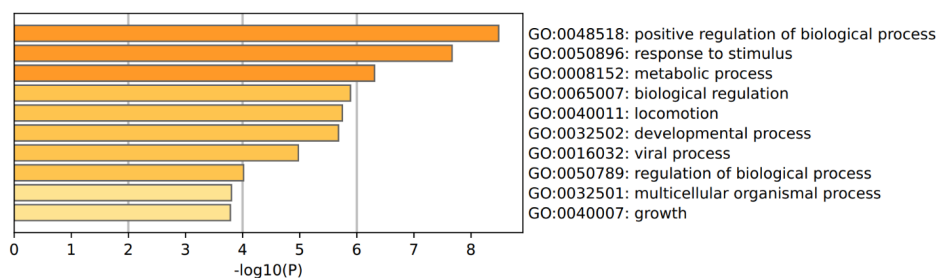


Figure 4. Heatmap-selected gene ontology (GO), revealing disease interactions, disease-related biological processes, responses, and metabolic pathways identified through GO analysis.

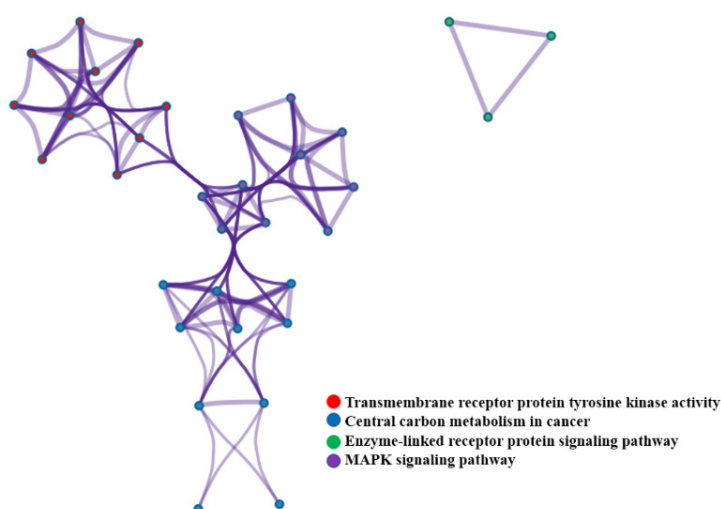


Figure 5. Enrichment gene ontology (GO) network associations, unveiling the connections within a specific group of genes or proteins.

The BOILED-EGG approach is used for predicting the bioavailability and pharmacological properties of a compound based on physicochemical descriptors (Figure 6). The white area indicates that plucheoside and syringaresinol have distinct physicochemical characteristics compared to pinosresinol. The blue color on the BOILED-EGG signifies that these three compounds

have associations with P-glycoprotein involved in the transportation of compounds across cell membranes and influence their bioavailability in the body. The homology modeling results are promising, as indicated by the Q-Mean Z-Scores, which are shown in blue (Figure 7).

The molecular docking simulation was first conducted by searching for the protein using the UniProt code

Table 1. Properties of absorption, distribution, metabolism, and excretion (ADME) of investigated compounds

ADME Properties	Pinosresinol	Syringaresinol	Plucheoside A
Molecular weight (g/mol)	358.39	418.44	412.47
Number of rotatable bonds	4	6	3
Number of hydrogen bond acceptors	6	8	8
Number of hydrogen bond donors	2	2	4
Molar refractivity (Å ²)	94.9	107.89	103.87
Topological polar surface area	77.38	95.84	125.68
Log P (Consensus)	2.26	2.33	0.63
Solubility	Soluble	Soluble	Soluble
Gastrointestinal absorption	High	High	High
Blood-brain barrier permeant	Yes	No	No
P-glycoprotein substrate	Yes	Yes	Yes
CYP2D6 inhibitor	Yes	Yes	No
CYP3A4 inhibitor	Yes	No	No
Lipinski	Yes	Yes	Yes

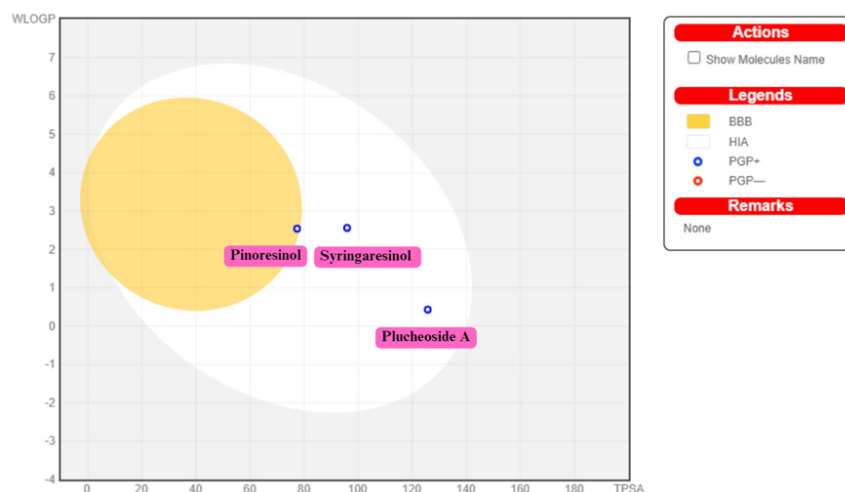


Figure 6. The estimation of bioavailability via brain or intestinal permeation assessments.

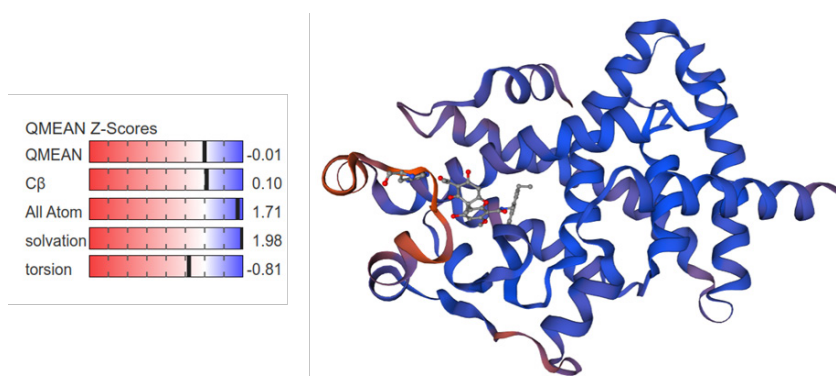


Figure 7. Image of protein results from homology modeling and validation.

P37231. From the data, one protein data bank with native ligands suitable for oriented docking was obtained. Root mean square deviation (RMSD) calculation for the protein (with PDB ID: 1FM9 in chain D) resulted in a value of 1.63. For Protein PDB (ID: 5F19), the obtained value was 0.72. RMSD was used to measure the difference between the position of the ligand from crystallography results and docking simulation. Additionally, it was used in comparing the original binding shapes (Figure 8). The results of the molecular docking studies showed that the target protein had the strongest interaction with its native ligand, which had the most negative binding energy (-12.62 kcal/mol) and the highest CNN pose score (0.93). In contrast, pinoresinol (-4.01 kcal/mol, CNN pose score

Table 2. Results of molecular docking showing binding energy and convolutional neural network (CNN) pose score

Compound	Binding energy (kcal/mol)	CNN pose score
Native ligand	-12.62	0.93
Pinoresinol	-4.01	0.55
Syringaresinol	-5.49	0.32
Plucheoside A	-4.19	0.44

0.55), syringaresinol (-5.49 kcal/mol, CNN pose score 0.32), and plucheoside A (-4.19 kcal/mol, CNN pose score 0.44) showed weaker interactions (Table 2).

The RMSD values of all compounds exhibited stability, with movements ranging from 0.1 to 0.25 nm. Additionally, molecular dynamics simulations confirmed the stability of these compounds, further validating their consistent behavior over time within the specified range (Figure 9). Meanwhile, Native ligand fell within the range of 0.1 to 0.28 nm and plucheoside A experienced atomic movements between 0.1 to 0.2 nm.

Figure 10 presents the results of the root mean square fluctuation (RMSF) calculation, which shows variations in specific amino acids. For the pinoresinol molecule, the highest variation occurred in Ile267, with a fluctuation magnitude of up to 0.2916 nm. In the case of syringaresinol, protein fluctuations were observed in Tyr477, reaching 0.5185 nm, while plucheoside A exhibited the largest fluctuation in Pro206, measuring 0.3898 nm.

The free energy binding of a native ligand and three compounds was subsequently computed using molecular dynamics and the molecular mechanics-generalized

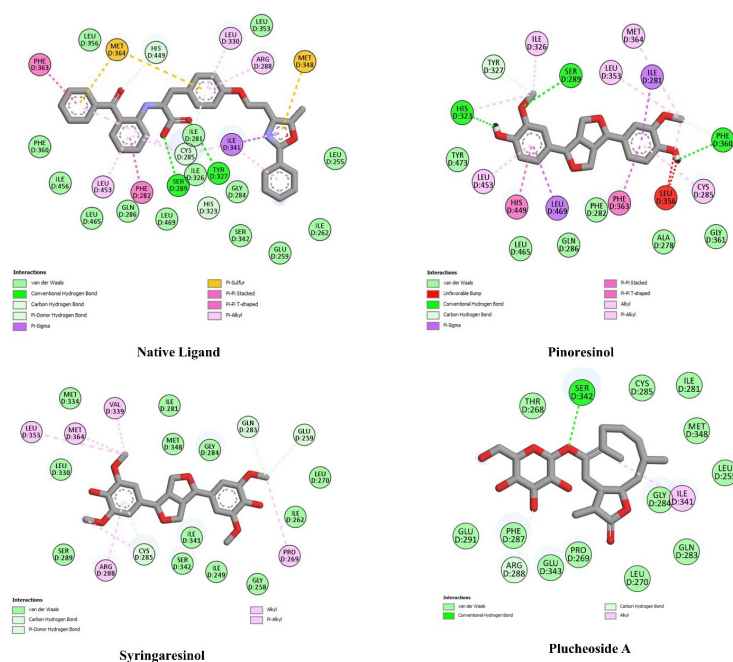


Figure 8. Interaction between PPARG with native ligand, pinoresinol, syringaresinol, and plucheoside A (PDB ID:1FM9).

Born and surface area (MM-GBSA) calculation method (Table 3).

Discussion

Three bioactive substances were derived from *P. indica*, specifically pinoresinol, syringaresinol, and plucheoside. Pinoresinol has been shown to interact with several target proteins in humans, including the enzymes arachidonate 5-lipoxygenase and prostaglandin G/H synthase 2 (PTGS2), transcription factors peroxisome proliferator-activated receptor alpha (PPARA), peroxisome proliferator-activated receptor delta (PPARD), and PPARG. Pinoresinol also interacts with unclassified proteins such as Rac GTPase-activating protein 1 (RACGAP1) and ATPase family AAA domain-containing

protein 5 (ATAD5). Syringaresinol is known to interact with the transcription factor PPARD and the enzyme DNA topoisomerase 1 (TOP1) [12]. The KEGG pathway database was also used to understand the relationship between diseases and pathways, encompassing genes, proteins, and metabolites (Figure 3) (33).

The network involving PPARA, PPARD, and PPARG was found to be associated with the known PPAR signaling pathway. Additionally, the network comprising PTGS2 and ALOX5 was related to the established arachidonic acid metabolism pathway and ovarian steroidogenesis. TOP1 was associated with ATAD5, an interaction supported by experimental data. However, no association existed between TOP1-ATAD5, PPARA-PPARD-PPARG, and the ALOX5-PTGS2 network. The lack of connections implies

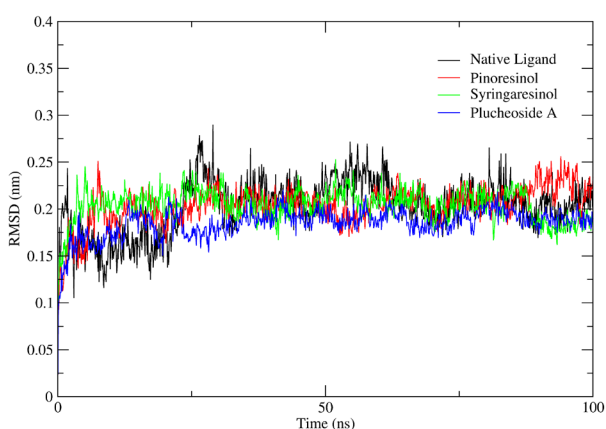


Figure 9. The root mean square deviation (RMSD) plot showing conformational changes of native ligand, pinoresinol, syringaresinol, and plucheoside A.

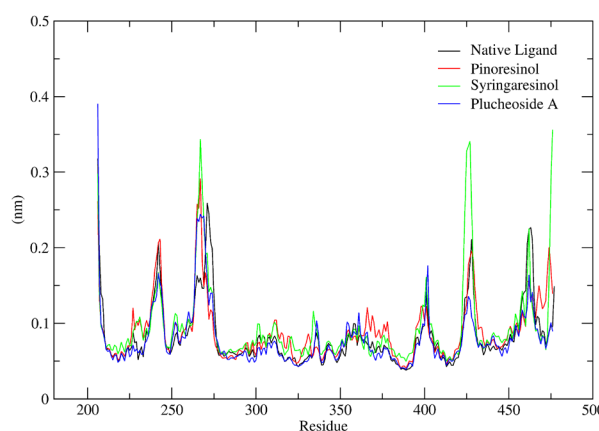


Figure 10. The root mean square fluctuation (RMSF) plots showing the flexibility of PPARG for each residue with native ligand, pinoresinol, syringaresinol, and plucheoside A.

Table 3. Free binding energy score using MM-GBSA method

Compounds	ΔG (kcal/mol)
Native Ligand	-70.23 \pm 3.48
Pinoresinol	-44.39 \pm 0.89
Syringaresinol	-51.83 \pm 13.31
Plucheoside A	-40.27 \pm 5.48

that the specific proteins are not related to PPAR signaling, arachidonic acid metabolism, or ovarian steroidogenesis pathways.

The relationship between diseases and proteins can be analyzed through text mining, which involves the use of the natural language processing method to extract information about disease-protein interactions from scientific literature. The results obtained included the proteins Insulin receptor (INSR), Epidermal growth factor receptor (EGFR), Ret proto-oncogene (RET), tumor protein p53, and Fibroblast growth factor receptor 1 (FGFR1), which exhibited relational connections. Experimental data and co-expression interactions were also found in INSR, EGFR, RET, and FGFR1. Co-expression refers to the simultaneous expression of two or more genes within the same cell or tissue, serving as a strong indicator of their functional relationship due to involvement in similar biological processes. This network is suitable for identifying potential drug targets, comprehending the molecular basis of diseases, and designing experiments to study gene functions.

The results illustrated that the polar surface area values were below 140 Å². This value is considered a recommended threshold for good oral absorption (34). Additionally, these three compounds are water-soluble and easily absorbed by the body, functioning as substrates of the P-gp protein transporter and inhibitors of the CYP2D6 enzyme. However, Plucheoside A among these compounds cannot penetrate the blood-brain barrier. Another aspect evaluated *in silico* was the potential toxicity based on the presence of toxicophore groups in the selected compounds. This evaluation was conducted using the SWISSADME and ADMETlab 2.0 web servers. The toxicophore criteria used were based on the structural alert rules defined by Brenk et al (35) as well as FAF-Drugs4 (36). Based on the results, the compounds Pinoresinol and Syringaresinol have a potentially problematic fragment, namely the phenol group. According to FAF-Drugs4 criteria, phenolic groups are classified as being potentially toxic due to their ability to generate free radicals that can damage DNA material. The biotransformation of phenolics yields electrophilic compounds having similar effects within the human body system. However, these results cannot be definitively drawn as conclusive, because numerous phenolic compounds are bioactive and beneficial to biological systems.

The BOILED-EGG approach showed two color-coded sections namely white and yellow (Figure 6). Pinoresinol

was positioned on the Egg graph with a yellow color, representing the blood-brain barrier. The yellow region on the Egg graph indicates that Pinoresinol possesses characteristics suggesting potential penetration across the blood-brain barrier. PPARG has interactions with SIRT1, NCOR2, PPAGCA1, CREBBP, MED1, NCOA1, NCOA2, RXRA, NCOR1, and RELA. KEGG analysis shows that the gene contributes significantly to the thyroid hormone pathway with a score of 1.127x10⁷. This indicates that *P. indica* may have potential in treatments that correlate with thyroid disease, as shown in Figure 3c.

Based on these outcomes, the regulatory functions involved in disease interaction include positive regulation of biological processes, response to stimulus, and metabolic processes. These are directly related to the PPAR signaling pathway (37).

Figure 5 illustrates the associations among the transmembrane receptor protein tyrosine kinase activities. Transmembrane receptor protein tyrosine kinases play a crucial role in cellular activities and processes such as growth, division, and metabolism. Understanding the mechanisms of these receptors could provide new insights into anti-cancer therapies (38).

Homology modeling was conducted due to the unsatisfactory quality of the validation for PDB ID 1FM9 in terms of its percentile ranks. The results showed the QMEAN Z-Scores, which depicted the resemblance of the constructed model to experimental results. The closer the value to zero, the better the alignment with experimental outcomes. Furthermore, the model was assessed based on C β , all-atom, solvation, and torsion, all of which indicated favorable outcomes, as shown in Figure 7. As the black line moved toward the right, the quality improved.

Redocking was performed to observe the RMSD value. RMSD can evaluate the accuracy of docking simulations and identify the most favorable binding positions, with the reference value being <2 (30). The docking analysis revealed varying degrees of interaction between different compounds and the target receptor (39). The docking results for PDB ID 1FM9 (Chain D) (presented in Table 2) showed that in the protein complex, the native ligand possessed a binding energy of -12.62 kcal/mol, indicating a strong interaction with the target protein. Moreover, the native ligand also achieved the highest CNN pose score of 0.93, signifying a favorable positioning within the protein binding site. Pinoresinol had a higher binding energy (-4.05 kcal/mol), although it was still lower than Syringaresinol (-5.49 kcal/mol) and Plucheoside A (-4.19 kcal/mol). The CNN pose score for Pinoresinol remained relatively high (0.55), indicating a fairly good placement.

The interaction between PPARG and active compounds presented in Figure 8 showed that Pinoresinol formed hydrogen bonds with the amino acids Ser289, His323, and Phe360, while Pi interactions occurred with His449, Phe363, Leu469, and Ile281. Syringaresinol exhibited

2 hydrogen bonds with Gln283, Glu259, and Cys285. Meanwhile, Plucheoside A featured 2 hydrogen bonds with Ser342 and Arg288, as well as one alkyl bond with Ile341.

Analysis using Discovery Studio showed that the active site residues included Cys285, Gly284, Phe282, Ser289, Met348, Ile341, Leu330, His449, Tyr473, and Met364. Additionally, the active configuration on PPARG involved the amino acids Asn450, Leu451, Ser452, Ser454, and Leu455 (20). The knowledge of the active site is crucial as it relates to chemical reactions and interactions.

The RMSD results from molecular dynamic simulations indicated that all active compounds derived from *P. indica* remained stable within the PPARG protein throughout the 100 ns simulation, as depicted in Figure 9 compared with the native ligand. The RMSF values indicated that for the Pinosresinol molecule, the highest variation occurred in Ile267 and Tyr477, while for Plucheoside A, the largest fluctuation was observed in Pro206. This indicates that the amino acids exhibit a high degree of flexibility in their movement during the molecular dynamic simulations.

The calculation of ΔG (delta G) using the MM-GBSA method is employed to predict the binding free energy between two molecules, such as a ligand and a receptor in molecular dynamics studies (Table 3). This method computes the contribution of energies from different interaction forces, including molecular mechanical energy (MM), solvation energy (GB), and the energy contribution from changes in surface area (SA). The three ΔG values provide information about the stability and relative interactions of these compounds within their environment. Lower values generally indicate that the interactions are more stable and thermodynamically favorable. Pinosresinol had the lowest value with a low uncertainty level, in comparison to the other compounds. This computation assessed polar solvation energy, which pertained to how molecules interacted with solvents and involved optimization calculations to yield accurate results (40).

Conclusion

Three active compounds were isolated from *P. indica*: pinosresinol, syringaresinol, and plucheoside A. These compounds were analyzed to meet the criteria of orally absorbable drugs. Network analysis demonstrated the potential of *P. indica* in treating medications for diabetes, regulation of thyroid hormones, adjustment of transmembrane receptor protein tyrosine kinase activity, intervention in cancer, and control of the MAPK signaling pathway. The molecular docking results exhibited a binding energy of -5.49 kcal/mol and a deep learning-based pose score of 0.32 for syringaresinol, indicating its strong interaction with the target protein. Additionally, this compound formed hydrogen bonds with the active site at amino acid Cys285. The molecular dynamics results

indicated that all active compounds derived from *P. indica* remained stable within the PPARG protein during the 100 ns simulation. Furthermore, Free energy calculations using MM-GBSA for all frames yielded ΔG values from -51.83 to -40.27 kcal/mol. It indicates the potential for the development drug as a target for PPARG.

Acknowledgment

We sincerely appreciate the support, guidance, and financial assistance the Faculty of Pharmacy Universitas Andalas .

Authors' contribution

Funding acquisition: Purnawan Pontana Putra, Dini Hanifa, Netty Suharti.

Investigation: Purnawan Pontana Putra, Raden Bayu Indradi, Tegar Achsendo Yuniarta, Dini Hanifa, Mokhamad Fahmi Rizki Syaban, Netty Suharti.

Methodology: Purnawan Pontana Putra, Raden Bayu Indradi, Tegar Achsendo Yuniarta, Mokhamad Fahmi Rizki Syaban.

Project administration: Purnawan Pontana Putra, Dini Hanifa, Netty Suharti.

Software: Purnawan Pontana Putra, Raden Bayu Indradi, Tegar Achsendo Yuniarta, Mokhamad Fahmi Rizki Syaban.

Validation: Purnawan Pontana Putra, Raden Bayu Indradi, Tegar Achsendo Yuniarta, Mokhamad Fahmi Rizki Syaban .

Visualization: Purnawan Pontana Putra, Raden Bayu Indradi, Mokhamad Fahmi Rizki Syaban.

Writing–original draft: Purnawan Pontana Putra, Raden Bayu Indradi, Tegar Achsendo Yuniarta, Dini Hanifa, Mokhamad Fahmi Rizki Syaban.

Writing–review & editing: Purnawan Pontana Putra, Raden Bayu Indradi, Tegar Achsendo Yuniarta, Dini Hanifa, Mokhamad Fahmi Rizki Syaban, Netty Suharti.

Conflict of interests

The authors affirm that there are no conflicts of interest in connection with this research.

Ethical considerations

This study followed ethical principles and standards and did not involve the participation of animals or humans. Instead, it primarily utilized computational and in silico methods such as network pharmacology, ADME prediction, deep learning docking, and molecular dynamics simulations.

Funding/Support

This research was generously funded by the Faculty of Pharmacy Universitas Andalas under the contract number 19/UN16.10.D/PJ.01./2023.

References

1. Kao CL, Cho J, Lee YZ, Cheng YB, Chien CY, Hwang CF, et al. Ethanolic extracts of *Pluchea indica* induce apoptosis and antiproliferation effects in human nasopharyngeal carcinoma cells. *Molecules*. 2015;20(6):11508-23. doi: 10.3390/molecules200611508.
2. Chan EW, Ng YK, Wong SK, Chan HT. *Pluchea indica*: an updated review of its botany, uses, bioactive compounds and pharmacological properties. *Pharm Sci Asia*. 2022;49(1):77-85. doi: 10.29090/psa.2022.01.21.113.

3. Sirichaiwetchakoon K, Churproong S, Kupittayanant S, Eumkeb G. The effect of *Pluchea indica* (L.) Less. tea on blood glucose and lipid profile in people with prediabetes: a randomized clinical trial. *J Altern Complement Med*. 2021;27(8):669-77. doi: 10.1089/acm.2020.0246.
4. Sirichaiwetchakoon K, Lowe GM, Thumanu K, Eumkeb G. The effect of *Pluchea indica* (L.) Less. tea on adipogenesis in 3T3-L1 adipocytes and lipase activity. *Evid Based Complement Alternat Med*. 2018;2018:4108787. doi: 10.1155/2018/4108787.
5. Ibrahim SR, Bagalagel AA, Diriri RM, Noor AO, Bakhsh HT, Mohamed GA. Phytoconstituents and pharmacological activities of Indian camphorweed (*Pluchea indica*): a multi-potential medicinal plant of nutritional and ethnomedicinal importance. *Molecules*. 2022;27(8):2383. doi: 10.3390/molecules27082383.
6. Zhang Y, Zhan RX, Chen JQ, Gao Y, Chen L, Kong Y, et al. Pharmacological activation of PPAR gamma ameliorates vascular endothelial insulin resistance via a non-canonical PPAR gamma-dependent nuclear factor-kappa B trans-repression pathway. *Eur J Pharmacol*. 2015;754:41-51. doi: 10.1016/j.ejphar.2015.02.004.
7. Janani C, Ranjitha Kumari BD. PPAR gamma gene-a review. *Diabetes Metab Syndr*. 2015;9(1):46-50. doi: 10.1016/j.dsx.2014.09.015.
8. Iawsipo P, Poonbud R, Somtragool N, Mutapat P, Meejom A. *Pluchea indica* tea-leaf extracts exert anti-cancer activity by inducing ROS-mediated cytotoxicity on breast and cervical cancer cells. *Br Food J*. 2022;124(12):4769-81. doi: 10.1108/bfj-05-2021-0497.
9. Sirichaiwetchakoon K, Lowe GM, Eumkeb G. The free radical scavenging and anti-isolated human LDL oxidation activities of *Pluchea indica* (L.) Less. tea compared to green tea (*Camellia sinensis*). *Biomed Res Int*. 2020;2020:4183643. doi: 10.1155/2020/4183643.
10. Noor F, Tahir UI Qamar M, Ashfaq UA, Albutti A, Alwashmi AS, Aljasir MA. Network pharmacology approach for medicinal plants: review and assessment. *Pharmaceuticals (Basel)*. 2022;15(5):572. doi: 10.3390/ph15050572.
11. Muhammad J, Khan A, Ali A, Fang L, Yanjing W, Xu Q, et al. Network pharmacology: exploring the resources and methodologies. *Curr Top Med Chem*. 2018;18(12):949-64. doi: 10.2174/1568026618666180330141351.
12. Gentile F, Agrawal V, Hsing M, Ton AT, Ban F, Norinder U, et al. Deep docking: a deep learning platform for augmentation of structure-based drug discovery. *ACS Cent Sci*. 2020;6(6):939-49. doi: 10.1021/acscentsci.0c00229.
13. Jiménez-Luna J, Grisoni F, Weskamp N, Schneider G. Artificial intelligence in drug discovery: recent advances and future perspectives. *Expert Opin Drug Discov*. 2021;16(9):949-59. doi: 10.1080/17460441.2021.1909567.
14. Szklarczyk D, Gable AL, Lyon D, Junge A, Wyder S, Huerta-Cepas J, et al. STRING v11: protein-protein association networks with increased coverage, supporting functional discovery in genome-wide experimental datasets. *Nucleic Acids Res*. 2019;47(D1):D607-13. doi: 10.1093/nar/gky1131.
15. Indradi RB, Pitaloka DA, Suryani. Network pharmacology to uncover potential anti-inflammatory and immunomodulatory constituents in *Curcuma longa* rhizome as complementary treatment in COVID-19. *Pharmacia*. 2022;69(4):995-1003. doi: 10.3897/pharmacia.69.e89799.
16. Zhou Y, Zhou B, Pache L, Chang M, Khodabakhshi AH, Tanaseichuk O, et al. Metascape provides a biologist-oriented resource for the analysis of systems-level datasets. *Nat Commun*. 2019;10(1):1523. doi: 10.1038/s41467-019-09234-6.
17. Daina A, Zoete V. A boiled-egg to predict gastrointestinal absorption and brain penetration of small molecules. *ChemMedChem*. 2016;11(11):1117-21. doi: 10.1002/cmdc.201600182.
18. Daina A, Michielin O, Zoete V. SwissADME: a free web tool to evaluate pharmacokinetics, drug-likeness and medicinal chemistry friendliness of small molecules. *Sci Rep*. 2017;7:42717. doi: 10.1038/srep42717.
19. Xiong G, Wu Z, Yi J, Fu L, Yang Z, Hsieh C, et al. ADMETlab 2.0: an integrated online platform for accurate and comprehensive predictions of ADMET properties. *Nucleic Acids Res*. 2021;49(W1):W5-14. doi: 10.1093/nar/gkab255.
20. Gampe RT Jr, Montana VG, Lambert MH, Miller AB, Bledsoe RK, Milburn MV, et al. Asymmetry in the PPARgamma/RXRalpha crystal structure reveals the molecular basis of heterodimerization among nuclear receptors. *Mol Cell*. 2000;5(3):545-55. doi: 10.1016/s1097-2765(00)80448-7.
21. Waterhouse A, Bertoni M, Bienert S, Studer G, Tauriello G, Gumienny R, et al. SWISS-MODEL: homology modelling of protein structures and complexes. *Nucleic Acids Res*. 2018;46(W1):W296-303. doi: 10.1093/nar/gky427.
22. Hanwell MD, Curtis DE, Lonie DC, Vandermeersch T, Zurek E, Hutchison GR. Avogadro: an advanced semantic chemical editor, visualization, and analysis platform. *J Cheminform*. 2012;4(1):17. doi: 10.1186/1758-2946-4-17.
23. Putra PP, Asnawi A, Hamdayuni F, Arfan, Aman LO. Pharmacoinformatics analysis of *Morus macroura* for drug discovery and development. *Int J Appl Pharm*. 2024;16(1):111-7. doi: 10.22159/ijap.2024.v16s1.126.
24. Suharti N, Sari MR, Dillasamola D, Putra PP. In silico and in vitro study of the ethanol extract of the white garland-lily (*Hedychium coronarium* J. Koenig) as a tyrosinase inhibitor. *Trop J Nat Prod Res*. 2023;7(6):3125-9. doi: 10.26538/tjnpr/v7i6.9.
25. McNutt AT, Francoeur P, Aggarwal R, Masuda T, Meli R, Ragoza M, et al. GNINA 1.0: molecular docking with deep learning. *J Cheminform*. 2021;13(1):43. doi: 10.1186/s13321-021-00522-2.
26. Lee J, Cheng X, Swails JM, Yeom MS, Eastman PK, Lemkul JA, et al. CHARMM-GUI input generator for NAMD, GROMACS, AMBER, OpenMM, and CHARMM/OpenMM simulations using the CHARMM36 additive force field. *J Chem Theory Comput*. 2016;12(1):405-13. doi: 10.1021/acs.jctc.5b00935.
27. Tian C, Kasavajhala K, Belfon KA, Raguette L, Huang H, Migués AN, et al. ff19SB: amino-acid-specific protein backbone parameters trained against quantum mechanics energy surfaces in solution. *J Chem Theory Comput*. 2020;16(1):528-52. doi: 10.1021/acs.jctc.9b00591.
28. Gao Y, Lee J, Smith IPS, Lee H, Kim S, Qi Y, et al. CHARMM-GUI supports hydrogen mass repartitioning and different protonation states of phosphates in lipopolysaccharides. *J Chem Inf Model*. 2021;61(2):831-9. doi: 10.1021/acs.jcim.0c01360.

29. Abraham MJ, Murtola T, Schulz R, Páll S, Smith JC, Hess B, et al. GROMACS: high performance molecular simulations through multi-level parallelism from laptops to supercomputers. *SoftwareX*. 2015;1-2:19-25. doi: 10.1016/j.softx.2015.06.001.
30. Rahim F, Putra PP, Ismed F, Putra AE, Lucida H. Molecular dynamics, docking and prediction of absorption, distribution, metabolism and excretion of lycopene as protein inhibitor of Bcl2 and DNMT1. *Trop J Nat Prod Res*. 2023;7(7):3439-44.
31. Miller BR 3rd, McGee TD Jr, Swails JM, Homeyer N, Gohlke H, Roitberg AE. MMPBSA.py: an efficient program for end-state free energy calculations. *J Chem Theory Comput*. 2012;8(9):3314-21. doi: 10.1021/ct300418h.
32. Valdés-Tresanco MS, Valdés-Tresanco ME, Valiente PA, Moreno E. gmx_MMPBSA: a new tool to perform end-state free energy calculations with GROMACS. *J Chem Theory Comput*. 2021;17(10):6281-91. doi: 10.1021/acs.jctc.1c00645.
33. Kanehisa M, Sato Y, Furumichi M, Morishima K, Tanabe M. New approach for understanding genome variations in KEGG. *Nucleic Acids Res*. 2019;47(D1):D590-5. doi: 10.1093/nar/gky962.
34. Shityakov S, Neuhaus W, Dandekar T, Förster C. Analysing molecular polar surface descriptors to predict blood-brain barrier permeation. *Int J Comput Biol Drug Des*. 2013;6(1-2):146-56. doi: 10.1504/ijcbdd.2013.052195.
35. Brenk R, Schipani A, James D, Krasowski A, Gilbert IH, Frearson J, et al. Lessons learnt from assembling screening libraries for drug discovery for neglected diseases. *ChemMedChem*. 2008;3(3):435-44. doi: 10.1002/cmdc.200700139.
36. Lagorce D, Bouslama L, Becot J, Miteva MA, Villoutreix BO. FAF-Drugs4: free ADME-tox filtering computations for chemical biology and early stages drug discovery. *Bioinformatics*. 2017;33(22):3658-60. doi: 10.1093/bioinformatics/btx491.
37. Kim T, Yang Q. Peroxisome-proliferator-activated receptors regulate redox signaling in the cardiovascular system. *World J Cardiol*. 2013;5(6):164-74. doi: 10.4330/wjc.v5.i6.164.
38. Du Z, Lovly CM. Mechanisms of receptor tyrosine kinase activation in cancer. *Mol Cancer*. 2018;17(1):58. doi: 10.1186/s12943-018-0782-4.
39. Handayani D, Aminah I, Pontana Putra P, Eka Putra A, Arbain D, Satriawan H, et al. The depsidones from marine sponge-derived fungus *Aspergillus unguis* IB151 as an anti-MRSA agent: molecular docking, pharmacokinetics analysis, and molecular dynamic simulation studies. *Saudi Pharm J*. 2023;31(9):101744. doi: 10.1016/j.jsps.2023.101744.
40. Wang E, Sun H, Wang J, Wang Z, Liu H, Zhang JZH, et al. End-point binding free energy calculation with MM/PBSA and MM/GBSA: strategies and applications in drug design. *Chem Rev*. 2019;119(16):9478-508. doi: 10.1021/acs.chemrev.

Copyright © 2024 The Author(s). This is an open-access article distributed under the terms of the Creative Commons Attribution License (<http://creativecommons.org/licenses/by/4.0>), which permits unrestricted use, distribution, and reproduction in any medium, provided the original work is properly cited.